# SOLAR X-RAY BURSTS AT ENERGIES LESS THAN 10 keV OBSERVED WITH OSO-4

J. L. CULHANE and K. J. H. PHILLIPS
*Mullard Space Science Laboratory, Dept. of Physics, University College, London*

(Received 25 August, 1969)

**Abstract.** Using data from a proportional counter spectrometer, sensitive in the wavelength range 1–20 Å, on OSO-4, X-ray bursts in the energy band 3.0 to 4.5 keV have been studied. 150 events have been identified between October 27, 1967 and May 8, 1968, mostly of an impulsive nature. Some gradual rise and fall bursts occur, but there is a selection bias against such long-enduring events. A study of the profiles of these events reveals no basis for identifying different types of impulsive event.

Single frequency radio bursts and Hα flares of class > 1F are almost always accompanied by X-ray enhancements. For the sample of X-ray events, only 25% are correlated with radio bursts and 46% with flares. Only 11% of the sample events are associated with type III radio bursts. Microwave burst peaks occur an average of two minutes earlier than the X-ray burst peak, but the first observation of X-ray activity is usually before the start of the corresponding microwave burst.

Impulsive bursts, although differing widely in fall time, are due to the heating of a volume of plasma from a temperature of 10.0 to $30.0 \times 10^6$ K. Differences in fall time probably indicate different electron densities in the source. Observation of an iron line at 1.9 Å suggests that a non-thermal mechanism may be operating during some of these events since the temperatures are too low to permit thermal excitation of the $1s^2$–$1s\,2p$ transition in $Fe^{+24}$. It is also possible that, in spite of the low temperature, most of the iron ions have been stripped to the $Fe^{+24}$ stage. Collisional excitation and dielectronic recombination processes would then be able to provide the observed flux in the resonance line of $Fe^{+24}$. A gradual rise and fall event and event 'precursors' have also been studied.

## 1. Introduction

Solar X-ray bursts have been observed at energies below 10 keV by many experiments flown on rockets and satellites. Much of the earlier work with broad band detectors (ion chambers and Geiger counters) was carried out by the NRL group (Acton *et al.*, 1963; Friedman, 1964). At energies above 20 keV, balloon borne instruments (Peterson and Winckler, 1959) and more recently experiments carried on spacecraft (Frost, 1964, Arnoldy *et al.*, 1968) have observed the hard X-ray bursts.

The two types of X-ray bursts have been described by De Jager (1964) as Quasi-thermal ($E \lesssim 10$ keV) and Non-thermal ($E \gtrsim 10$ keV). The present work deals entirely with quasi-thermal events at photon energies below 10 keV. Although the decay of the flux following the event peaks appears due to the cooling of a plasma, there is evidence that the 1.9 Å line in Iron (Neupert *et al.*, 1969; Meekins *et al.*, 1968) is non-thermally excited during some events or that the population of the $Fe^{+24}$ stage is anomalously high.

X-ray event counting rate profiles were examined in order to provide a basis for classifying the events. The occurrence of X-ray bursts was correlated with other solar phenomena. Impulsive bursts, gradual rise and fall bursts and event precursor features have been studied and the nature of the emitting regions is discussed in each case. A

number of plasma cooling mechanisms are examined in the case of the impulsive bursts.

## 2. The X-Ray Spectrometer

The instrument is located in one of the wheel compartments of the OSO-4 spacecraft. A brief description is presented here since a more detailed discussion has already been published (Culhane *et al.*, 1967). Seven proportional counter detectors are used. Their properties are summarised in Table I. Detectors are connected in sequence to an eight channel differential pulse height analyser. An eight channel solar spectrum and a background measurement are obtained from each detector in a time of less than four seconds so a spectrum in the range 1–18 Å is obtained every fifteen seconds together with an indication of the flux level in the 44–60 Å band. Pairs of detectors (B and C, D and E) of different sensitivity are employed in the wavelength range below 10 Å. When the solar flux rises, the lower sensitivity detector of the pair is automatically selected. This enables large flares to be studied while minimising the effects due to detector saturation. The detectors and the pulse handling circuits are calibrated 'on board' with the aid of radioactive Iron-55 sources. Photons from the sources are admitted to the detectors in response to a command which operates four shutter carrying solenoids.

TABLE I

The proportional counter parameters

| Identification | Wavelength range (Å) | Dimensions (mm) | Gas filling 1 atm | Window | |
|---|---|---|---|---|---|
| | | | | Material | Thickness |
| A | 6–18 | Cylindrical 22.2 diam. 139.3 length | 90% Neon 10% Carbon Dioxide | Aluminium | 1.35 mg cm$^{-2}$ |
| B | 3–9 High Sensitivity | Cylindrical 31.75 diam. 175.0 length | 90% Neon 10% Carbon Dioxide | Beryllium | 13.5 mg cm$^{-2}$ |
| C | 3–9 Low Sensitivity | Cylindrical 31.75 diam. 167.2 length | 90% Neon 10% Carbon Dioxide | Beryllium | 22.5 mg cm$^{-2}$ |
| D | 1–3 High Sensitivity | Disc-End Window 60.0 diam. 24.0 thickness | 90% Argon 10% Carbon Dioxide | Beryllium | 91.4 mg cm$^{-2}$ |
| D* | Anticoincidence with D output | Within volume defined above for D | As in D | No X-ray window | |
| F and G | 44–56 | Cylindrical 9.5 diam. 97.0 length | 90% Argon 10% Carbon Dioxide | Melinex<br>Aluminium | 0.52 mg cm$^{-2}$<br>0.041 mg cm$^{-2}$ |
| E | 1–3 | Cylindrical 22.2 diam. 116.4 length | 90% Argon 10% Carbon Dioxide | Beryllium | 91.3 mg cm$^{-2}$ |

The spectrometer began operation on October 23, 1967 and is continuing to give good data up to the present time. Solar coverage has never been complete, averaging between 50% and 60% each day while the spacecraft tape recorders continued to operate. Data loss is enforced by the shadowing of the spacecraft by the Earth, by tape recorder playback periods and by transits through the South Atlantic Magnetic Anomaly. Data obtained during 'anomaly' transits is ignored because of the increased background counting rate due to trapped radiation. The solar coverage was reduced from about 60% to 15% per day after the failure, on May 12th 1968, of the second spacecraft tape recorder. The X-ray bursts discussed in the present paper were obtained from 'quick look' records over the period October 23, 1967 to May 8, 1968. During this period, the detectors sensitive at wavelengths below 18 Å have maintained their gains to within 2% of the prelaunch figures. The normal background counting rate for the system lies between 0.3 and 1.5 counts per pulse height channel per second.

In order to obtain information about the source function, the energy resolution of the detectors must be considered. Monoenergetic photons, absorbed in a proportional counter, give rise to a pulse height distribution of near Gaussian form. The standard deviation of such a distribution is given by the expression

$$\sigma = kE^a \tag{1}$$

where $E$ is the photon energy in keV and $k$ and $a$ are constants for a particular detector. We have tried a number of iterative methods for unfolding the detector resolution but these methods must be used with caution particularly when spectra have been obtained during solar flares (Culhane *et al.*, 1969). In the present study, we have computed the response of detectors D and E to a continuum source function of the form

$$I_\lambda \propto \exp\left[-\frac{hc}{\lambda kT}\right]\frac{\bar{g}(\lambda, T)}{\lambda^2} \tag{2}$$

where $\bar{g}$ $(\gamma, T)$ is a Free-Free Gaunt factor obtained by fitting an expression to the results of Karzas and Latter (1961).

The temperature is determined from the ratio of the counting rates in a pair of adjacent channels. In view of the small number of lines observed during flares at wavelengths below 5 Å (Meekins *et al.*, 1968), it is possible to pick a pair of channels which do not contain any strong lines. The temperature determined is thus a good estimate of the source temperature. Hudson *et al.* (1969) have also established temperatures in this way. The escape peak correction was not applied in calculating these relations. Since the counter filling gas is Argon and the source spectra are steep, the neglect of this effect will not lead to significant errors. Line emission is significant at wavelengths longer than 5 Å, so it is not possible to obtain source temperature by calculating the response of the longer wavelength detectors to the continuum source function alone.

A strong line has been observed at around 1.9 Å by the crystal spectrometer ex-

periments of Meekins *et al.* (1968) and Neupert *et al.* (1969). This feature can be detected by our 1–3 Å detectors (D and E) during some X-ray events. Following Fritz *et al.* (1969), we employ the parameter

$$R = \frac{C_p - \frac{C_{p-1} + C_{p+1}}{2}}{\frac{C_{p-1} + C_{p+1}}{2}} \tag{3}$$

as an experimental measure of the line flux. $C_p$ represents the observed counting rate in the pulse height channel which contains the line. If $C_L$ is the counting rate in the $p$th channel produced by a line at 1.9 Å (6.5 keV) and $C_c$ is the counting rate in the same channel due to the continuum source function, then for a given temperature $T$, the parameter $R$ may be calculated as a function of the ratio $C_L/C_c$. In this way values of the Iron line to continuum ratio may be estimated from experimentally determined values of $R$.

## 3. The Identification of X-Ray Events and their Properties

The 'quick look' data records provided about 120 min of solar data each day for the period October 23, 1967 to May 8, 1968. X-ray events or short term enhancements in the solar X-ray flux were identified in the data from these records and their parameters were measured. A total of 150 events were identified and the paper deals with the study of the parameters of these events, their correlation with other solar phenomena and with the detailed properties of a small number of representative events.

### 3.1. The Selection of X-Ray Events

An X-ray event was identified as a short term enhancement in the counting rate profile obtained from the first channel of either of the 1–3 Å detectors (D or E). These detectors cover a 3:1 range in photon energy and the boundaries at channel one, although slightly different for the two detectors, are set to register photons in the energy range 3.0 to 4.5 keV. The sensitivity of detector E is a factor 16 lower than that of detector D.

The channel one counting rates were plotted against time and events were selected using the following criteria:

1. The peak counting rate observed during the course of the event was more than three standard deviations above the steady counting rate or baseline.
2. The whole event was delineated by a sequence of at least five points.
3. The whole event was visible on the counting rate plot of data from one daylight pass of 60 min duration.

Point (2) above ensured that no event of duration less than 90 sec was selected. Point (3) resulted in a bias against long duration events with a cut off at a duration of 60 min. No attempt has yet been made to correct for this bias, but more complete

data are now available on magnetic tape records and we hope to correct this sample of events in the near future. Because of the bias against long duration events, most of the events in the sample will be of an impulsive character although there is some evidence for the existence of X-ray events of the 'gradual rise and fall' type.

### 3.2. Event parameters

After the identification of an event, in accordance with the criteria given in Section 3.1, a number of event parameters were measured from the counting rate against time profile. The parameters were as follows: –

1. The universal time of the event peak.
2. The 10% to 90% rise time ($t_R$).
3. The 10% to 90% fall time ($t_F$).
4. The total duration of the event measured between points at 10% of the peak value ($t_D$).
5. The difference between the peak counting rate and the pre-event counting rate ($\Delta\phi$).

Many of the quoted event times were determined from the 'quick look' records with the aid of the times of day to night transition as listed in the spacecraft world maps. Such times have an uncertainty of $\pm$ 1 min. In the case of those events correlated with radio phenomena and for about half the events correlated with H$\alpha$ flares, peak times were determined with an accuracy of a few seconds with the aid of the magnetic tape records which became available during the course of the study.

The rising and falling parts of the event counting rate profiles are approximately exponential in shape. This was also established by Hudson *et al.* (1969) for events at photon energies above 7.7 keV. Events have been detected with both the high and low sensitivity detectors (D and E). Values of $\Delta\phi$ have been corrected by a factor equal to the ratio of the detector window areas so that all values are referred to detector D.

### 3.3. A study of the event parameters

The study was undertaken in order to find a basis for classifying X-ray events. It was hoped that such a classification would give some insight into the production of intermediate energy X-rays during such events.

Plots of burst intensity against duration have been used by Covington (1959) to classify solar microwave radio events. A plot of his data for a sample of 2800 MHz microwave bursts shows two well-developed prongs corresponding to simple impulsive bursts and gradual rise and fall bursts. Figure 1 shows a similar diagram for the 150 X-ray events of the present study. There is slight evidence for the existence of a lower prong, but because of the bias against long duration events, this prong is not well developed. The eighteen events that appear to define the prong are ringed. Events have been observed that are very similar to radio gradual rise and fall events. A profile (plot of X-ray counting rate against time) for one such event is presented in Figure 16.

With the exception of the eighteen events provisionally designated as gradual rise and fall, the events in the sample are impulsive in character. Their properties were studied in an attempt to identify different types of impulsive event. Histograms of all the events, in increments of rise and fall time, were plotted. Both histograms vary smoothly with rise times having a tighter distribution than fall times. The typical

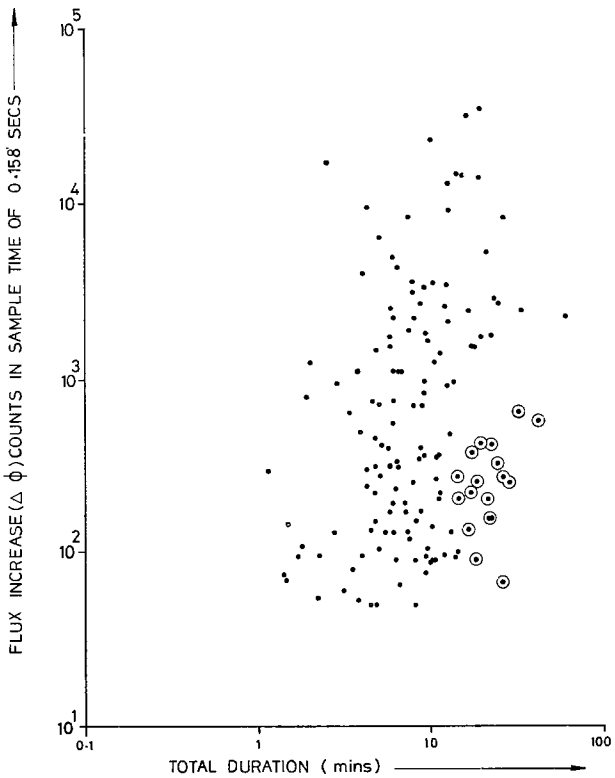


Fig. 1. Scatter diagram of 150 X-ray bursts. Log of counting rate increase ($\Delta\phi$) versus log of duration ($t_D$).

event of the sample has an asymmetric profile with a rise time of 2.8 min and a fall time of 6.3 min. The histograms show no structure and give no evidence for the existence of different classes of impulsive event.

A histogram of all the events in increments of an asymmetry parameter ($S=t_F/t_R$) was also plotted. Again no structure is apparent; the sample shows a smooth variation from events with symmetric profiles to events with rapid rise times and slow fall times.

The 150 events have been divided into groups consisting of the 75 largest events and the 75 smallest events. There is no significant difference between the rise time, fall time and total duration histograms for these two groups. The distributions in $S$ differ slightly but just significantly. It may be seen in Figure 2 that the smaller events exhibit

a somewhat more pronounced symmetry than the larger. However, the third distribution given in Figure 2 results when the smaller 'gradual rise and fall' events are removed. Since these events tend to be symmetric, the difference disappears. This provides support for the identification of gradual rise and fall events.

If the total number of events is divided about a value of $S$ equal to 2.0, an almost

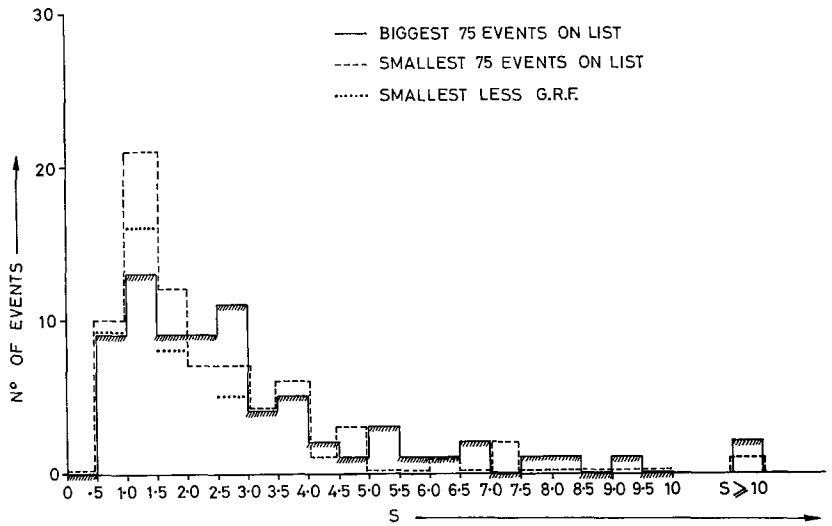


Fig. 2. Histograms of events in equal increments of the parameter $S$ ($S = t_F/t_R$).

equal number of events is found above and below this value. The more symmetrical events have a broader distribution of rise times than the asymmetric events. The removal of the gradual rise and fall events from these distributions does not change them significantly.

Rise times are plotted against fall times in Figure 3 for all the events. The points exhibit considerable scatter as do the points plotted by Hudson *et al.* (1969) at higher energies. Those events which are indicated in Figure 1 as belonging to a gradual rise and fall branch are also identified in Figure 3. They exhibit slower rise times than the majority.

While the examination of event parameters indicates that both impulsive and gradual rise and fall events exist at intermediate X-ray energies (3–4.5 keV), the sample of events is biased against the long duration events. We will attempt to reduce the effect of this bias with the more complete data available on magnetic tape records. There is no evidence for the existence of different types of impulsive event.

## 4. A Comparison of the X-Ray Events with other Solar Phenomena

The comparison of X-ray bursts with other solar phenomena is a necessary prelude to the understanding of the mechanisms involved. Several authors (including Arnoldy

*et al.* (1968), Neupert *et al.* (1969), Donnelly (1968), Teske (1969) and Hudson *et al.* (1969)) have recently compared X-ray burst observations with radio, optical and ionospheric data. A significant part of the earlier work has been reviewed by Kundu (1965).

The present study deals with the comparison of the intermediate energy (3–4.5 keV)

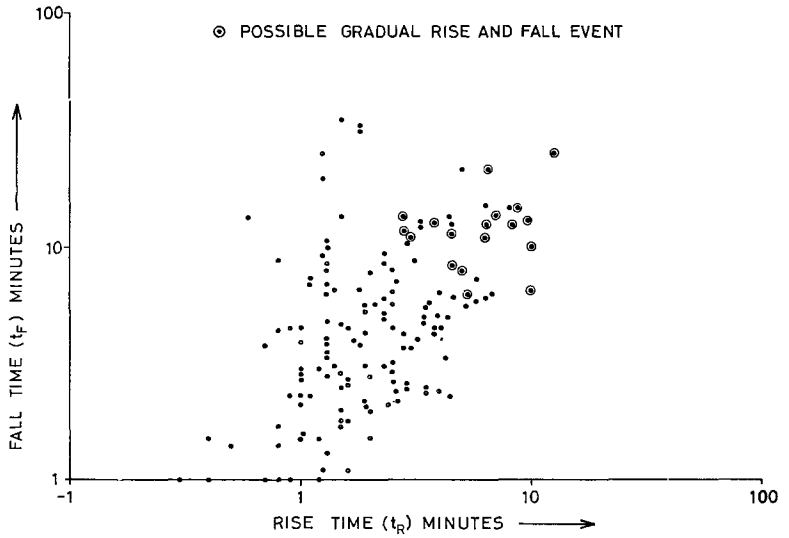


Fig. 3. Rise time ($t_R$) plotted against fall time ($t_F$) for 150 events.

X-ray bursts described in the previous section with some of the other phenomena listed above.

### 4.1. X-RAY BURSTS AND SINGLE FREQUENCY RADIO BURSTS

Details of single frequency radio events were obtained from *Solar Geophysical Data*, *IAU Bulletin on Solar Activity* and from the monthly or quarterly reports of the observing stations at Heinrich Hertz Institute, Manila, Nagoya, Nera, Penticton, Ottawa and Sagamore Hill. The observing frequencies were in the range 100 MHz to 10 000 MHz though almost all the events are visible and detectable at frequencies above 1000 MHz.

Table II shows details of the X-ray-radio correlations in both forward (i.e. X-ray events correlated with radio bursts) and reverse (radio bursts correlated with a significant X-ray enhancement) directions. Events were taken as correlated if their time-profiles overlapped. The forward correlation figure is very similar to that obtained by Hudson *et al.* (1969) for about the same number of X-ray events in the energy range 7.7 to 12.5 keV. The reverse correlation has been examined only up to December 31, 1967. In the period for which satellite X-ray data were available, only one radio event was found unaccompanied by an X-ray enhancement. Eleven events occurred at

TABLE II

X-ray-single frequency radio burst correlations

| Forward correlation | Number of X-ray events | Reverse correlation | Number of radio events |
|---|---|---|---|
| Oct. 23, 1967–May 8, 1968 | | Oct. 23, 1967–Dec. 31, 1967 | |
| No. of *X-ray* events observed in 'quick-look' records | 150 | No. of *radio* events (any frequency) observed during periods for which satellite 'quick look' records were available | 38 |
| *X-ray* event accompanied by radio event (any frequency) | 34 (23%) | *Radio* events any frequency accompanied by X-ray event | 26 (68%) |
| *X-ray* event accompanied by radio event (2800 MHz) | 26 (17%) | *Radio* event occurred during the tail of an X-ray event or at a time of high X-ray activity | 11 (29%) |
| *X-ray* event accompanied by radio GRF event or long enduring complex event (2800 MHz) | 10 (6.7%) | *Radio* event not accompanied by X-ray event ($f = 111$ MHz, Flux = 250 Units) | 1 (3%) |

*NOTE:* 11 *Radio* events at $f = 2800 \pm 300$ MHz were *all* accompanied by X-ray events.

times when the X-ray activity was high, making it difficult to recognise X-ray events. If we disregard these eleven events the reverse correlation is 95%. The one uncorrelated event is at a low frequency (see Table II). However, one other uncorrelated radio event occurred. On October 26, 1967, a small microwave impulse (5 flux units) was observed in the Nagoya record on 9400 MHz (Tanaka, 1968). The event was too brief to be included in the Nagoya report of outstanding events and so it has not been included in Table II. The X-ray observations around this time are discussed in more detail elsewhere (Culhane *et al.*, 1969). The 26 radio events that were accompanied by X-ray events extend down to 3–5 flux units at peak.

In the photon energy range 10–50 keV, Arnoldy *et al.* (1968) find that the peak X-ray flux is proportional to the peak microwave flux. This proportionality is not evident in our lower energy data. Figures 4 and 5 show the relationships between 3–4.5 keV and 1–1.5 keV X-ray peak fluxes and the peak flux of the associated radio event. A number of events, which were slightly affected by detector saturation, were omitted. Hudson *et al.* (1969) find a similar variability in the X-ray-radio peak flux relation. These findings differ from the result obtained by Teske (1969) whose data for the 8–12 Å band suggest a proportionality between soft X-ray and microwave peak fluxes.

We have examined the relative timing of the X-ray and microwave flux profiles. The peak of the 3–4.5 keV X-ray emission is delayed by an average time of two minutes with respect to the peak of the microwave flux. The distributions of time delay for events are shown in Figure 6. The scatter is less when radio GRF events are excluded and, with the exception of one doubtful correlation, the microwave peak occurs *before* the X-ray peak in all cases; Teske and Thomas (1969) find delays of three to six minutes

between the microwave peak and the 8–12 Å X-ray peak. Events for which we have studied counting rate profiles obtained by the long wavelength detectors show that the softer the radiation, the later the time at which the peak flux occurs, with a time difference of several minutes between the hardest and softest peak. A similar effect is observed by Neupert *et al.* (1969) who find that the higher excitation lines are en-

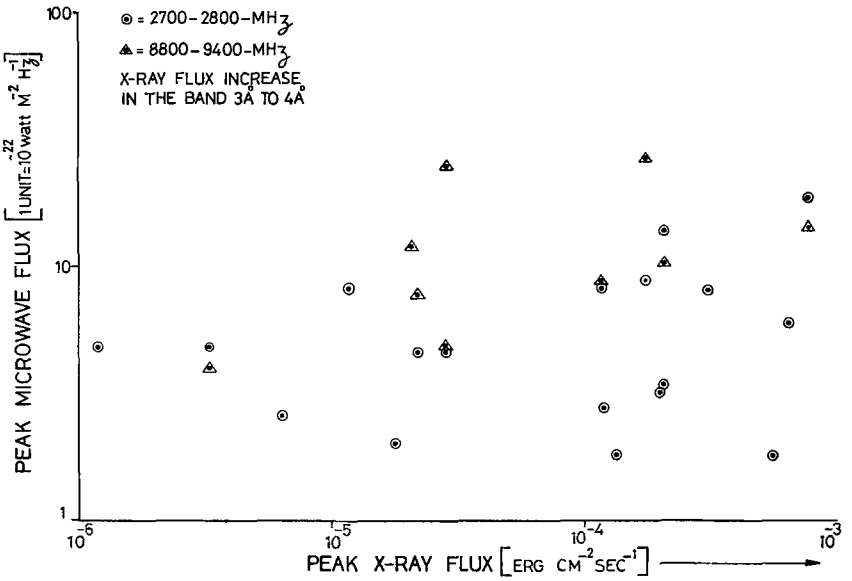


Fig. 4. Peak microwave flux plotted against peak X-ray flux in the 3–4 Å band for several microwave-correlated events.

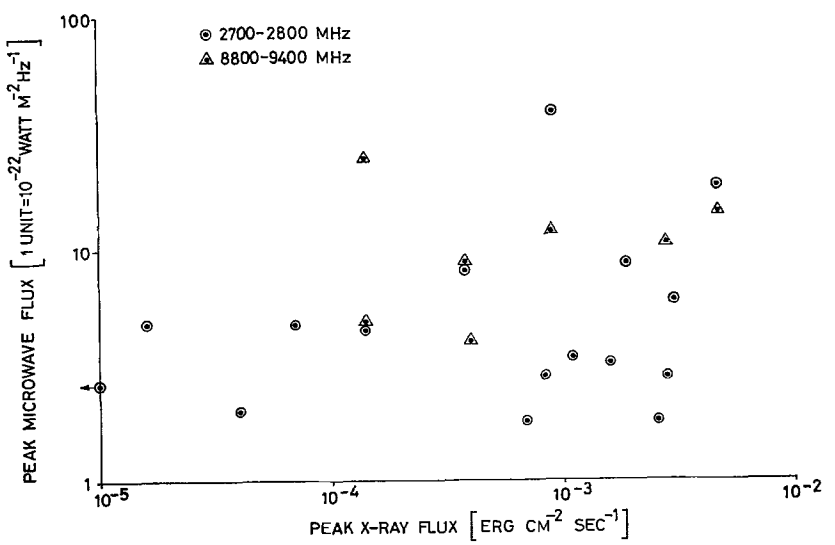


Fig. 5. Peak microwave flux plotted against peak X-ray flux in the 11–12 Å band for several microwave-correlated events.

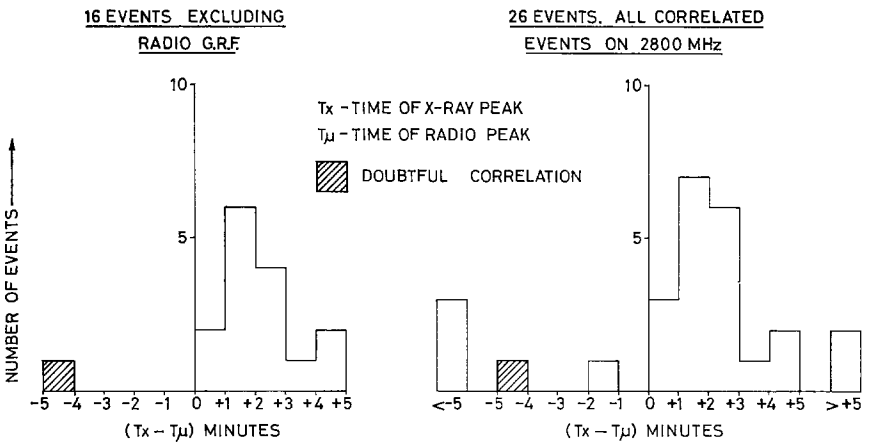


Fig. 6. Histograms of time difference ($T_x$–$T_\mu$) for X-ray events with correlated microwave emission on 2800 MHz.

hanced earlier than the lines of lower excitation. Arnoldy *et al.* (1968) find that the profiles of 10–50 keV events are very similar to the correlated microwave profiles. The higher energy photons ($E \gtrsim 10$ keV) are probably Bremsstrahlung produced by accelerated electrons while the softer photons ($E \lesssim 10$ keV) may arise from plasma that has been heated as a result of collisions with accelerated electrons or by some other mechanism. The details of the flare interaction may be established by careful studies of X-ray and radio event profiles at different energies, but the nature of the interplay of thermal and non-thermal processes is not well understood at present.

Although the peak of the soft X-ray flux occurs after the microwave peak, X-ray activity can frequently be detected before the start of the microwave burst and before the rapid rise of the X-ray profile. The event profiles shown in Figures 14 and 15 have small precursors. While such precursors are not invariably detected, they occur frequently. If we define the starting time of the X-ray event as the time when the counting rate profile first changes slope, then this time can precede the earliest reported microwave starting time by as much as fifteen minutes. Teske and Thomas (1969) have pointed out that the observation of preceding X-ray activity depends on the sensitivity of the X-ray detector. The association of precursor activity with the main event is complicated in our case by the restricted nature of the 'quick look' records, but observations made with our high sensitivity detector (detector D) show the same tendency for X-ray activity to precede the microwave activity as that noted by Teske and Thomas for the 8–12 Å band.

The relation between X-ray event and microwave event rise times is shown in Figure 7. The impulsive X-ray events have rise time that correlate well with those of the corresponding impulsive microwave events. The relation for 'Gradual Rise and Fall' microwave events is confused. The points representing four events appear to follow the relationship established from the impulsive events. In the case of the re-

maining four GRF radio events, it seems clear that impulsive X-ray events have been associated with gradual radio events.

### 4.2. X-RAY BURSTS AND TYPE III RADIO BURSTS

It has been suggested by Kundu (1965) that the relationship between hard X-ray events and fast drift radio bursts is not as close as that found between X-rays and single frequency bursts. Our observations at 3–4.5 keV point to a similar conclusion as do the observations of Hudson *et al.* (1969).

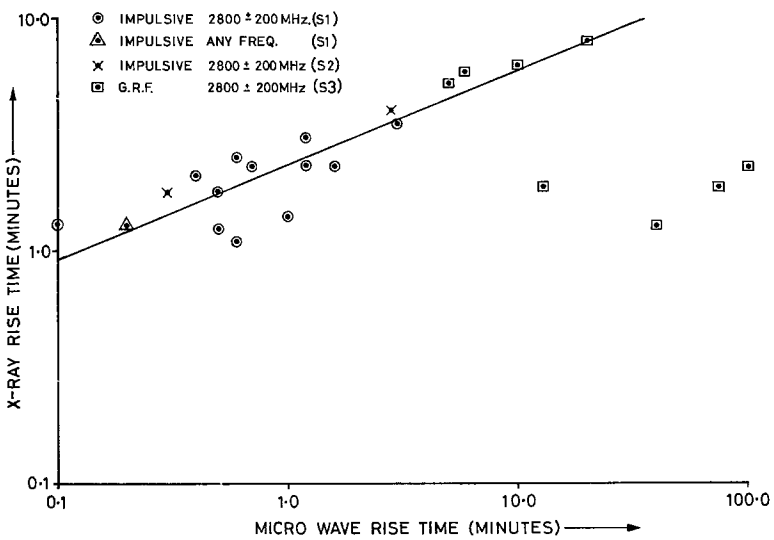


Fig. 7. Relation between X-ray event and microwave event rise time.

Table III gives details of the forward and reverse correlations. Because of the very short duration of the type III events, a correlation was also recognised if the time difference between the peak at the X-ray event and the middle of the type III event was less than 10 min. Although the percentage of forward correlations (21%) is about the same as for the single frequency events using this criterion, it is considerably less (11%) when an overlap is demanded. In addition, five type III events have been observed unaccompanied by X-ray events as against one single frequency radio event.

Histograms of the time difference between the peak of the X-ray event and the mid-point of the type III burst are given in Figure 8. While there is a tendency for the peak of the X-ray burst to follow the type III burst, it is not as marked as in the case of the X-ray to single frequency burst time difference. The histograms have been plotted using the two criteria mentioned in the preceding paragraph. These histograms are much broader than those of Figure 6, which further emphasises the looseness of the relationship.

While a more detailed study of the X-ray events, using instruments of better time

TABLE III

X-ray-type III burst correlation

| Forward correlation | Number of X-ray events | Reverse correlation | Number of Type III events |
|---|---|---|---|
| Oct. 23, 1967–May 8, 1968 | | Oct. 23, 1967–Dec. 31, 1967 | |
| No. of *X-ray* events observed in 'quick look' records | 150 | No. of *type III* events observed during periods for which "quick look" records are available | 42 |
| *X-ray* event accompanied by type III event (any frequency) | 17 (11%) | *Type III* event accompanied by X-ray event (10 minute criterion) | 29 (69%) |
| *X-ray* event peak within 10 minutes of type III burst centre | 32 (21%) | *Type III* event not accompanied by X-ray event (10 minute criterion) | 5 (12%) |
| | | *Type III* event occurred during tail of X-ray event or period of high X-ray activity | 8 (19%) |

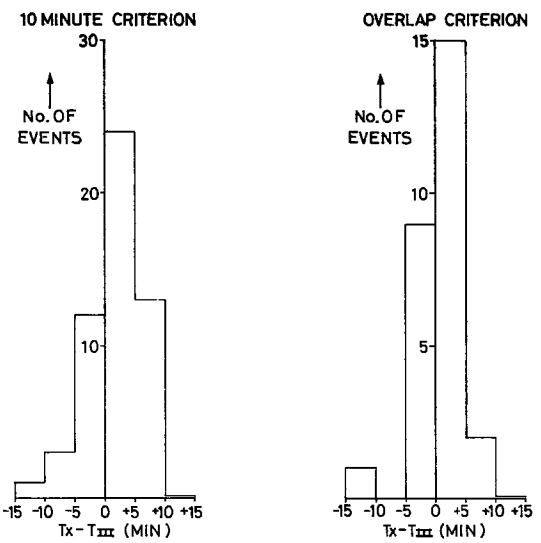


Fig. 8. Histograms of the time difference between X-ray peak time ($T_x$) and midpoint times of correlated type III radio bursts ($T_{III}$).

resolution, might show some relation between X-ray and type III bursts, the data already available suggest that this is not likely to be a very fruitful line of inquiry.

### 4.3. X-RAY BURSTS AND Hα FLARES

Although the Hα emitting regions of the solar atmosphere must exist under very different conditions from those prevailing in the X-ray regions, recent high resolution solar images obtained during the course of a flare by Vaiana *et al.* (1968) show that

the shape and extent of the Hα and X-ray emitting regions are very similar. This suggests an intimate connection between the phenomena.

Details of the correlation between Hα flares and the X-ray bursts observed by the OSO-4 instrument are given in Table IV. The flare times were obtained from the complete flare lists published in *Solar Geophysical Data.* More than half of the *X-ray events* were not accompanied by flares although only 18% of the *flares* in the reverse sample were not accompanied by significant X-ray enhancements. If we discount the five flares that occurred during an X-ray event or at times of high X-ray activity, all flares of class 1N or greater were accompanied by an X-ray enhancement.

TABLE IV

X-ray-Hα flare correlations

| Forward correlation | Number of X-ray events | Reverse correlation | Number of Hα flares |
|---|---|---|---|
| Oct. 23, 1967–May 8, 1968 | | Oct. 23, 1967–Dec. 31, 1967 | |
| No. of *X-ray* events observed in 'quick look' records | 150 | No. of *Flares* and *Sub-flares* observed during periods for which satellite 'quick look' records were available | 21 flares<br>190 sub-flares<br>Total: 211 |
| *X-ray* event accompanied by any type of flare or sub-flare | 69<br>(46%) | No. of *Flares* and *Sub-flares* correlated with X-ray enhancements | 138<br>(65%) |
| *X-ray* event not accompanied by any optical flare or sub-flare | 77<br>(51%) | No. of *Sub-flares* not correlated with X-ray enhancements | 39<br>(18%) |
| *X-ray* event during period of no flare patrol | 4<br>(3%) | No. of *Flares* and *Sub-flares* occurring during the tail of an X-ray event or at a time of high X-ray activity | 34<br>(16%) |

Of the 39 subflares not accompanied by X-ray emission, 30 were of class −F and 9 were of class −N.

The relation between peak X-ray flux and flare class is rather variable. While large Hα flares (class > 2N) are accompanied by large X-ray fluxes, subflares are frequently accompanied by X-ray events that are just as large. However, a small X-ray event is less likely to be accompanied by a flare. This is demonstrated in Figure 9 where the numbers of events in various X-ray flux ranges are displayed. A slight dependence of peak X-ray flux on measured flare area is shown by the data of Figure 10 but the scatter is considerable. The use of corrected flare areas, as listed in *Solar Geophysical Data*, leads to a plot with similar scatter.

Plage regions with McMath numbers 9034, 9073, 9115 and 9153 were found to be 'prolific' X-ray producers as compared to other regions (Teske and Thomas, 1969). These regions gave rise to 12 of the 150 X-ray events. These twelve events displayed a higher than average flux in the 3–4.5 keV band. For the twelve events from the 'prolific' regions, the average peak counting rate was 3.5 times greater than the average peak counting rate for all the events.

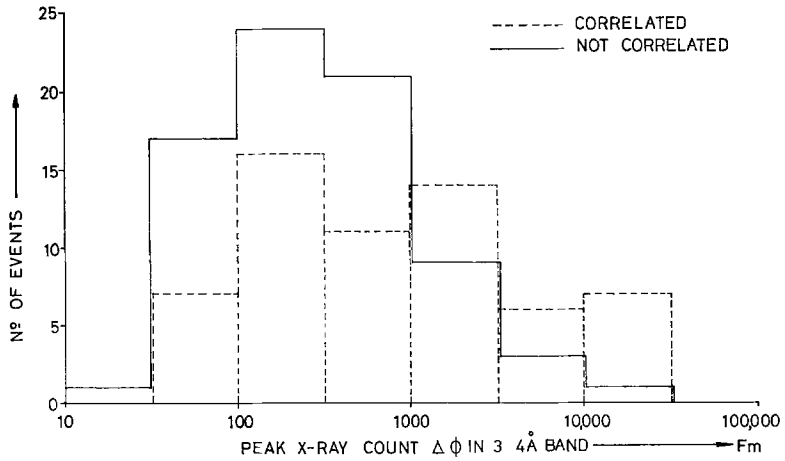


Fig. 9. Histograms of number of X-ray events correlated and not correlated with Hα flares.

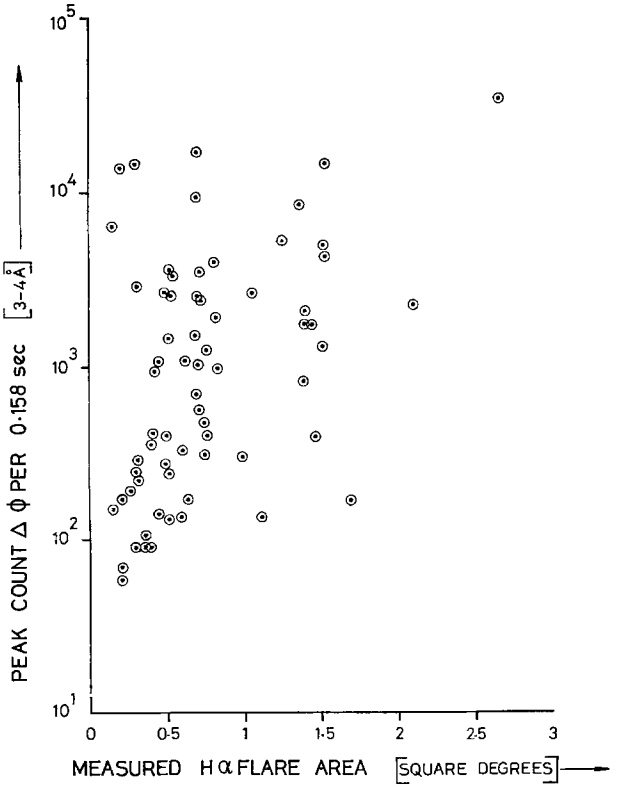


Fig. 10. Peak X-ray count ($\Delta\phi$) plotted against measured Hα flare area.

In comparing the times of occurrence of the X-ray and Hα peaks, the accuracy of the X-ray event timing must be discussed. Of the 69 X-ray events correlated with Hα flares, it proved impossible to determine the time difference in the case of seven of them. The distributions of time difference of the remaining 62 events are shown plotted in Figure 11 in two groups of 31 events each. For one group the events have

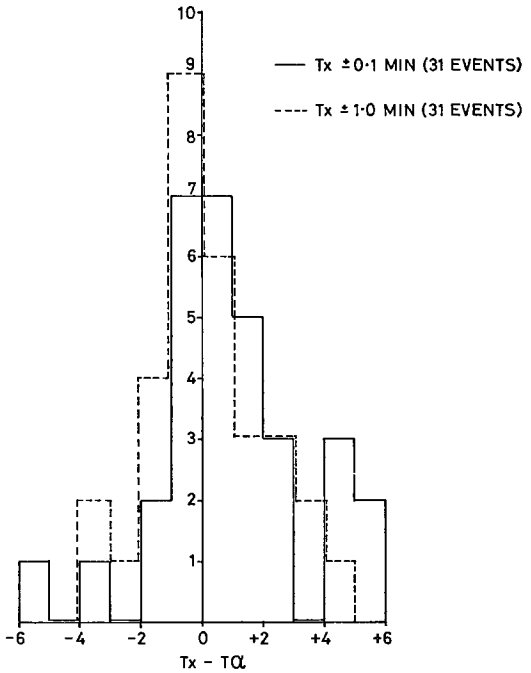


Fig. 11. Distribution of differences between X-ray and Hα flare peak times.

been timed very accurately with the aid of data from magnetic tape records; the events in the other group have been less accurately timed, but there is no significant difference between the two distributions. There is a much greater spread in these distributions than in the X-ray to microwave distribution with no obvious indication of the X-ray events occurring later. This may be partly due to the fact that the Hα-flare peaks are in some cases poorly defined.

The distributions of X-ray events with heliographic longitude have been plotted for three different longitude bin sizes. In each case there is a centre to limb decrease in the number of X-ray events that is just significant, as shown in Figure 12. Ken-Ichiro Ohki (1969) finds that X-ray bursts at energies greater than 10 keV show a similar effect while bursts at energies less than 6 keV show an essentially flat distribution with longitude. The bursts at less than 6 keV discussed by Ken-Ichiro Ohki were observed with a broad band detector (1–6 keV) by Van Allen (1967) while the present observations are confined to the 3–4.5 keV band. However, event radiation in both these bands is probably produced quasi-thermally in a hot plasma. The centre to

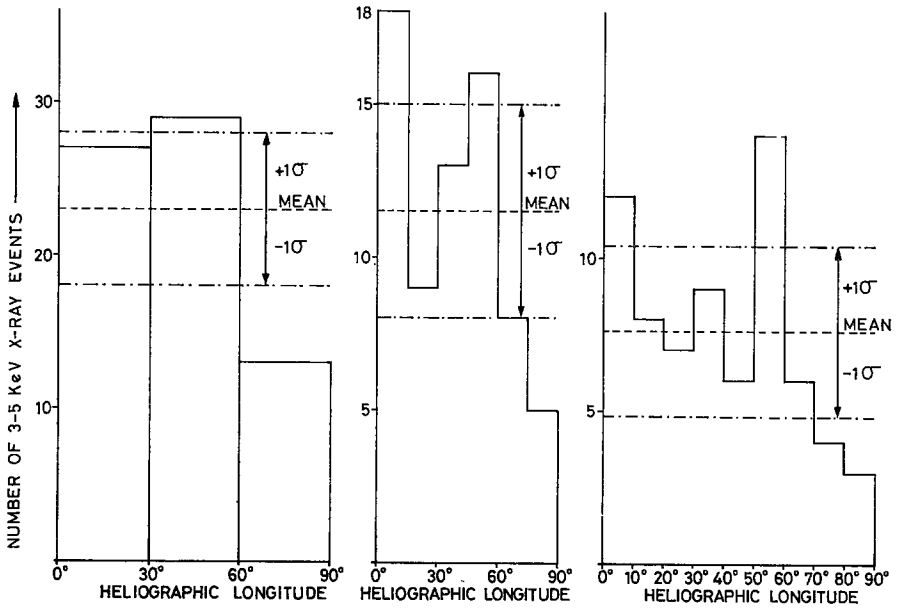


Fig. 12. Frequency of occurrence of Hα correlated X-ray events plotted against heliographic longitude.

limb variation in the 3–4.5 keV event frequency distribution is therefore unlikely to be due to the directivity of the X-radiation.

## 5. The Production of Soft X-Ray Bursts

In the previous sections, we have examined properties of the X-ray events themselves and their relationship with radio and optical phenomena.

Because of the bias against long duration events, the majority are classified as impulsive. X-ray bursts of the 'gradual rise and fall' (GRF) type have also been observed although the number of such bursts is not large. The two types of burst will be discussed separately. We have also remarked on the existence of pre-event or precursor X-ray activity before many of the impulsive events. The nature of this radiation will be briefly examined.

### 5.1. Impulsive bursts

Examination of the distributions of event parameters gives no evidence for the existence of different classes of impulsive event. There is instead a relatively smooth variation from the most impulsive events with symmetric profiles to less impulsive events with asymmetric profiles, i.e. with fast rise times and slow fall times. The profiles of two events, representing extremes of this variation, are shown in Figures 13 and 14. Both events are preceded by small enhancements or precursors. Although the form of such precursors is variable, they occur frequently.

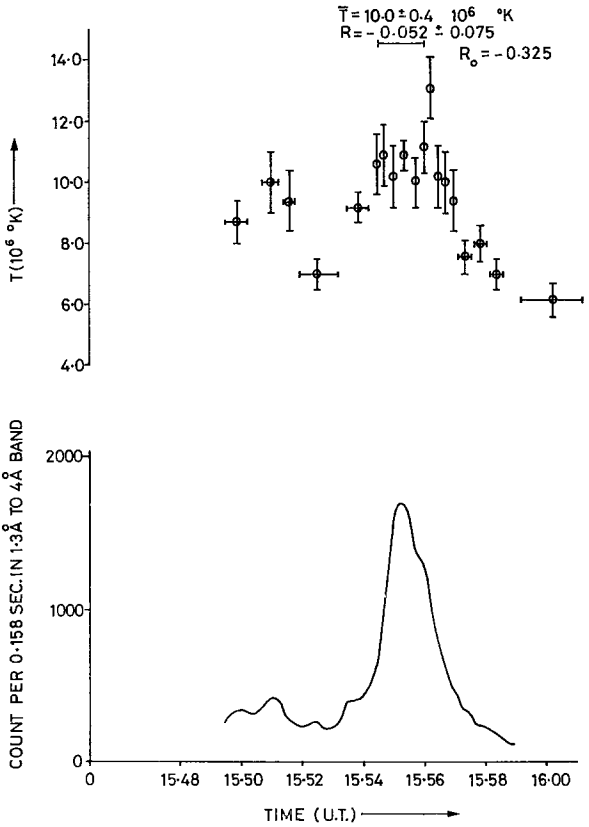


Fig. 13. Temperature and counting rate in the 1.3–3.9 Å band plotted against time for an event on January 23, 1968.

Takakura (1969) has recently discussed the production of X-rays during impulsive bursts. He suggests that both thermal (i.e. Maxwellian) and non-thermal electrons are required to radiate the observed X-rays by the Bremsstrahlung process. His comments apply to photon energies above 10 keV.

It has been suggested in the past (Culhane *et al.*, 1964) that, even at lower photon energies, the very impulsive X-ray events of short duration were due to Bremsstrahlung from non-thermal electrons. In the present study we have examined the events, using the methods of Takakura, in an attempt to establish which is the dominant process.

The event in Figure 13 occurred on January 23, 1968 at 15.55 UT. It has a nearly symmetrical profile in the 3–4 keV band ($S = 1.3$, see Section 3) and a duration of only four minutes. The peak flux was small enough for the event to be studied with the high sensitivity detector (D) without saturation effects. The counting rate profile in Figure 13 refers to the counting rate registered in the 1.3–3.9 Å band. The impulsive nature of the rise and decay sections of the event could give the impression that the non-thermal component of the X-ray Bremsstrahlung is significant, possibly even dominant, despite the low energy range (3–10 keV) covered by this detector.

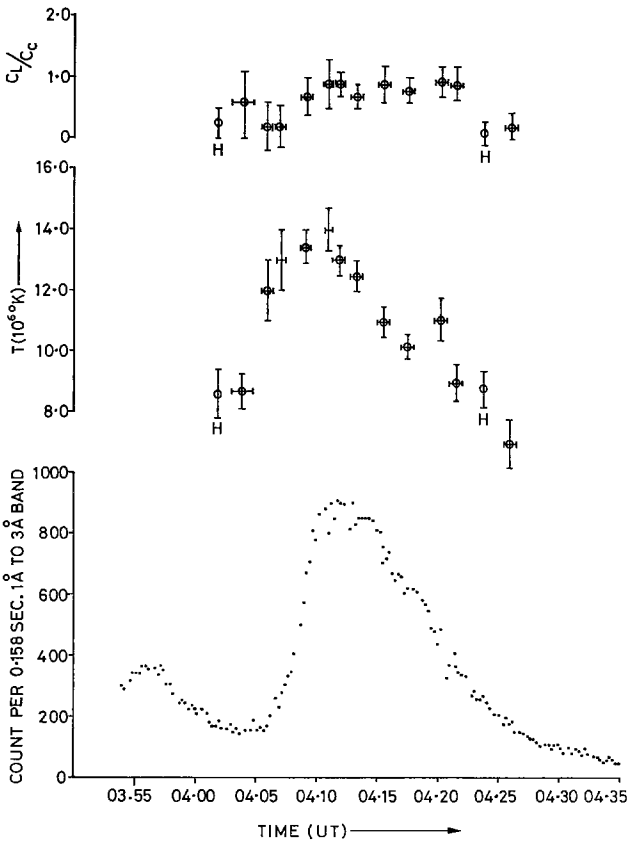


Fig. 14. Line-to-continuum ratio ($C_L/C_C$), temperature and counting rate in 1–3 Å band plotted against time for an event on October 27, 1967. Points obtained with high sensitivity detector are labelled 'H'.

Takakura's treatment consists in matching the observed flux decay with a model which assumes that the decay is due to time-variation of the energy distribution of the non-thermal electrons alone. This allows the product $Vg$ to be determined where $V$ is the emissive volume of the region and $g$ the constant in the electron energy distribution $n(e)\,de = g\,e^{-\gamma}\,de$. By assuming $V = 10^{29}$ cm$^3$, as Takakura does, the number density of non-thermal electrons is obtained. The value is typically $10^{-3}$ or $10^{-4}$ of the ambient plasma density in the events studied by Takakura and this restricts the range of possible solutions. For the event on January 23. 1968, matching a calculated flux decay profile with the profile observed leads to the following properties of the source region – ambient plasma density $= 10^{12}$ cm$^{-3}$, non-thermal electron density $5 \times 10^9$ cm$^{-3}$, $\gamma = 1.7$.

These results look improbable since the event is small, but requires a small value of $\gamma$ which should imply a large flare. Also, a very large flux from Iron characteristic radiation is predicted by the approximate treatment of Acton *et al.* (1963) of about

$7 \times 10^{-2}$ ergs cm$^{-2}$ sec$^{-1}$. Electrons in the range 10–30 keV are taken into account by Acton, but with a flat electron energy distribution, as is required in this case, a significant number of electrons have energies above 30 keV. Therefore the above estimate is a lower limit. Moreover, the Bremsstrahlung at $\lambda = 1.9$ Å is calculated to be $2 \times 10^{-2}$ erg cm$^{-2}$ sec$^{-1}$ Å$^{-1}$, about $10^3$ times greater than the observed values.

Such large discrepancies suggest that the soft X-ray burst on January 23, 1968 is not compatible with a non-thermal hypothesis as envisaged by Takakura. However, there is reason to suppose that a non-thermal component is still significant in producing the observed features, attributed to Fe, at a wavelength of about 1.9 Å. The line emission at this wavelength is barely significant during the event of January 23, 1968. The average value of $R$, determined between 01.54.30 UT and 01.56.00 is just three standard deviations greater than $R_0$, the value of $R$ that is consistent with zero line emission. During the second event, which occurred on October 27, 1967, the line is more easily detectable but the temperature attained at the peak of the event is only $14 \times 10^6$ K. The event is illustrated in Figure 14 where the counting rate (Detector E), temperatures and line to continuum ratio are plotted against time. The temperatures and line to continuum ratios were derived by taking ratios of counts in various channels as described in section 2 of the present paper. The decaying part of the counting rate profile is too slow to be matched with any theoretical curve for reasonable values of $\gamma$ and ambient plasma density.

Neither of these events can therefore be explained by Bremsstrahlung radiation from a power law electron spectrum extending to low electron energies. This conclusion agrees with the work of Takakura. His model predicts that, at low photon energies, radiation from the hot plasma will exceed the Bremsstrahlung flux from non-thermal electrons. However, the plasma temperatures at the peaks of the two events are less than $20.0 \times 10^6$ K and such low temperatures are not compatible with the thermal excitation of the $1s^2$–$1s\,2p$ transition in $Fe^{+24}$ (Culhane and Phillips, 1969). Therefore, some non-thermal excitation mechanism may be operating to produce the 1.9 Å Iron line which is observed during the October 27 event, although the presence of the line is barely significant during the January 23 event. If almost all the iron in the radiating volume were in the $Fe^{+24}$ stage, the observed line flux could be produced by a combination of electron collisional excitation and dielectronic recombination processes (Jordan, 1969). The number of ions in the $Fe^{+24}$ stage would therefore have to be considerably larger than the value obtained from an ionisation balance calculation at the observed temperature.

In the two events studied, the emission measure remains constant to within 20% during the falling parts of the counting rate profiles although it appears to increase in both cases. Hudson *et al.* (1969) report that the emission measure is conserved in a larger number of events. The drop in flux is therefore not likely to be caused by the loss of plasma from the emitting region. If we assume that the decrease in temperature, observed during the falling parts of both events, indicates a cooling plasma whose electrons have a Maxwellian velocity distribution, a number of cooling mechanisms may be considered.

The hot plasma may be isolated and cooled by radiation. We have calculated the radiative cooling rate, due to Free–Free, Free–Bound and line emission at wavelengths below 30 Å, as a function of temperature. Using these cooling rates, the time for a plasma to lose $1/e$ of its total energy may be calculated as a function of electron density for various initial temperatures. Cooling times can be estimated from the temperature measurements of Figures 13 and 14. The results are given in Table V.

TABLE V

Cooling mechanisms

| Event | Emission measure at time of peak flux $\int N_e^2 \, dV \, cm^{-3}$ | Electron density | | Source diameter (arc min assuming a spherical source) | |
|---|---|---|---|---|---|
| | | Radiation Cooling | Collisional cooling | Radiation cooling | Collisional cooling |
| January 23rd 1968 15.55 UT | $3.3 \times 10^{47}$ | $3.5 \times 10^{11}$ | $3.0 \times 10^{9}$ | 0.05 | 1.0 |
| October 27th 1968 04.11 UT | $1.8 \times 10^{48}$ | $9.0 \times 10^{10}$ | $9.0 \times 10^{8}$ | 0.17 | 3.7 |

If the heating of the plasma occurs in a short time, a significant difference may exist between the electron temperature and the ion temperature at the time of peak X-ray flux. The electrons can then lose energy by collision with the ions. A similar suggestion has been made by Hudson *et al.* Setting the event fall times equal to the electron-proton equipartition time of Spitzer (1962) we obtain the values of electron densities listed in the fourth column of Table V. These values are smaller than are obtained from the radiative model and lead to considerably larger volumes for the emitting regions.

Conduction from the emitting region also provides a possible energy loss mechanism (Vesecky, 1969). Unrestricted conductive loss through the entire boundary surface of the emitting region would result in a loss of energy in a time of milliseconds. Containment of the plasma in a magnetic field can inhibit conduction across the field lines. The relatively small energy loss due to conduction across the ends of the source may then be able to provide the observed event fall times. The forms of the X-ray emitting regions observed during a solar flare by Vaiana *et al.* (1968) suggest that such a mechanism may be possible. We will examine the various plasma cooling hypotheses in more detail in a future publication. Although a continuous distribution of symmetry is observed in the sample of events, with values of $S$ (Section 3) ranging from 1.0 to above 10.0, the nature of the events seems to be similar. For the impulsive events a volume of plasma is rapidly heated in a violent interaction during which the velocity distribution of the plasma electrons is non-Maxwellian. The gas then cools with the cooling time probably being set by the electron density in the source. Two extreme cooling models are presented. Observations of the sizes of the emitting regions, with

the ability to resolve diameters of less than 1.0 arc min, could allow the cooling mechanism to be identified.

### 5.2. Precursor features

As noted in Section 2, significant X-ray events are frequently preceded by small enhancements in X-ray activity. Precursors have also been observed by Hudson *et al.* (1969) in the 7–12 keV band and by Teske and Thomas (1969) in the 1–1.5 keV band.

Counting rate profiles from the three detectors are shown in Figure 15 for a period on October 24, 1967. The data points have been smoothed using a five point Gaussian filter. A well-marked precursor is evident in the 1–3 Å data but the increase is not so obvious in the case of the other two detectors. The small flux enhancement before the start of the main event is not always as well defined as is shown in Figure 15. In several cases there is a slow rise in flux followed by a fast rise without an inter-

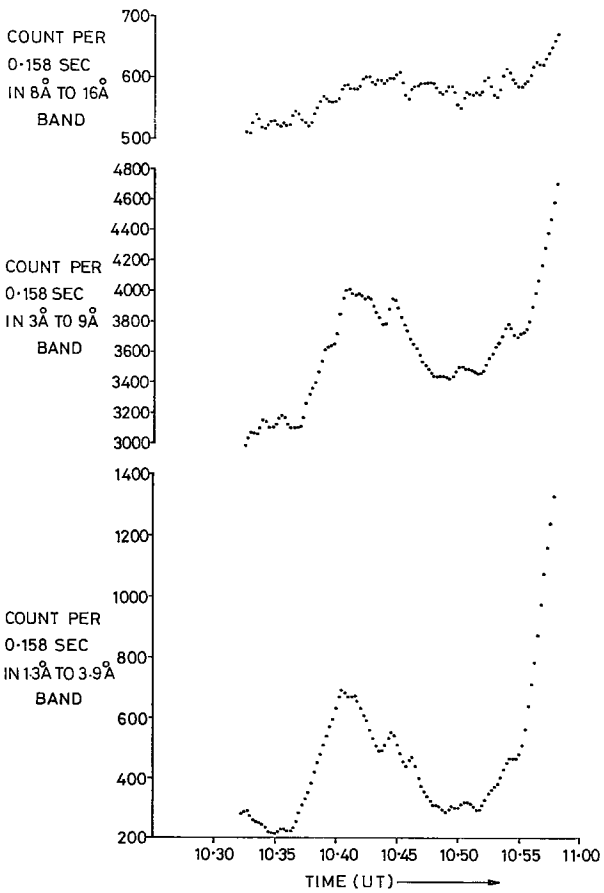


Fig. 15. Counting rates in 8–16 Å, 3–9 Å and 1.3–3.9 Å bands plotted against time for an event precursor on October 24, 1967.

mediate fall. The present discussion is confined to cases where a small rise and fall were observed before the main event.

For the October 24 event, a total of 17 count histograms, obtained during the period 10.32 UT to 10.36 UT before the start of the precursor were combined to provide an average count histogram. The channel 2 to channel 1 ratio from the average histogram yielded a temperature of $7.8 \pm 0.3 \times 10^6$ K. Since the instrument is sensitive to radiation from the whole Sun, care must be taken when deriving the properties of the region that emits the precursor radiation. If most of the radiation from the Sun is being emitted by the region where the precursor occurs, then the count histogram, obtained at the peak of the precursor, should provide details of the emitting region. If the pre-event radiation is coming from several different regions, it is necessary to subtract the pre-event histogram from the peak histogram in order to obtain information about the source of the radiation. Since there were several active regions on the Sun at the time of the observation, the latter course was adopted.

An average of 26 count histograms was taken for the period 10.40 UT to 10.45 UT. This average histogram is valid for the peak of the precursor. The average histogram, obtained before the event, was subtracted from the peak histogram and the resulting difference histogram yielded a temperature of $9.3 \pm 0.3 \times 10^6$ K. A comparison of the difference histogram with the calculated free–free and free–bound spectrum for a unit volume plasma at a temperature of $9.3 \times 10^6$ K gives an emission measure, $\int N_e^2 \, dV$, of $1.8 \times 10^{47}$ cm$^{-3}$ for the emitting region.

Kundu (1965) quotes the relations for the calculation of microwave radio flux from a plasma having (a) a large optical depth and (b) a small optical depth at centimetre wavelengths. If the X-ray emitting region is optically *thick* for microwave radiation, the observed temperature change of $1.5 \times 10^6$ K leads to an increase in flux of 0.5 W m$^{-2}$ Hz$^{-1}$ at 2800 MHz. A source diameter of 0.5 arc min was assumed in deriving this figure. In the optically *thin* case, the radio flux is a function of the emission measure and varies inversely with $T^{0.5}$. The observed temperature change would have produced a negligible decrease in radio flux. No increase in radio flux was reported during the period of the precursor. A simple microwave event was observed to begin at 10.50 UT on 3000 MHz at both the Nera and Heinrich Hertz radio observatories but no activity was reported by these stations before 10.50 UT on October 24.

A total of seven precursors has been examined including the event which occurred on October 24. The peak temperatures observed vary between $8.5 \times 10^6$ K and $10.5 \times 10^6$ K. The increase in temperature is around $2.0 \times 10^6$ K for all these events, so they are generally similar to the October 24 precursor discussed in the previous paragraph. No increases in radio flux were observed at the times of the X-ray precursors although several of the associated main events are correlated with microwave enhancements. From the absence of increases in radio flux we conclude that, for the precursor events observed, the emitting regions are either optically thin at radio wavelengths or, if optically thick, are smaller than 0.5 arc min in diameter.

Since the peak temperatures for all the precursor events lie within a $30 \times 10^6$ K range, a composite count histogram has been formed by adding together the peak histo-

grams from all the precursors. The temperature obtained from the channel 2 to channel 1 ratio is $10.0 \pm 0.1 \times 10^6$ K.

Iron line emission in the energy range 6.4 to 6.6 keV would contribute an excess count above the continuum mainly in channel 5. Using the sum of the peak histograms, the parameter $R$ (Section 2) is found equal to $-0.119 \pm 0.020$ while the use of the source function of Equation (2), with a temperature of $10.0 \times 10^6$ K and no line flux at 6.5 keV, leads to a calculated value of $R$ ($Ro$) of $-0.327$. The measured value of $R$ therefore differs by about ten times the RMS statistical error from the value that is consistent with no line emission. The measured value of $R$ leads to a value of $0.70 \pm 0.10$ for the ratio of line produced counts at 6.5 keV to continuum produced counts in the 0.8 keV energy interval of channel 5. If the temperature, determined from the channel 2 to channel 1 ratio, is in error, there will be an additional error in the line to continuum ratio, but it would require an increase of $40.0 \times 10^6$ in this temperature for the observed value of $R$ to be consistent with zero line flux.

It appears therefore that, even during the precursor features, this high excitation line is produced.

### 5.3. Gradual rise and fall bursts

The sample of events contains very few of this type because of the bias against finding long duration events that was mentioned in Section 3. One such burst was observed on February 2, 1968 between 06.43 UT and 07.30 UT. Counting rate profiles from three of the detectors during this period are presented in Figure 16. The flux increase in the 1–3 Å band is considerably larger than that observed in the 3–9 Å band while the increase in the 8–16 Å band is only 25% of the pre-event level. Bursts of this kind have been observed by Hudson *et al.*, but their examples generally exhibit less symmetrical profiles than the event shown in Figure 16. This category of burst is also recognised by White (1964), but the profile of the sample event presented in this paper lacks symmetry and is very similar to the event shown in Figure 14.

Average count histograms were obtained from the detector E data for a number of periods during the course of the event. Temperature could be determined more accurately with the aid of the high sensitivity detector. The temperature, measured at the beginning of the event, has been established with data from both detectors, but for consistency the low sensitivity detector has been used throughout. The peak temperature was obtained by subtracting the first histogram from the peak histogram and taking the channel 1 to channel 2 ratio from the difference histogram. A temperature of $11.5 \pm 0.5 \times 10^6$ K was established for the peak of the event while the temperature at the start of the event was $8.7 \pm 0.4 \times 10^6$ K. The temperature rises gradually from this value to the peak value in time of 20 minutes and then falls slowly in about the same time. The value of the parameter $R$, obtained from a sum of 30 histograms around the peak of the event, was consistent with zero iron line emission at 6.5 keV. By comparing the flux values obtained from the difference histogram with the calculated thermal continuum flux from a unit coronal volume at $11.0 \times 10^6$ K, we obtain an emission measure, $\int N_e^2 \, dV$, of $1.5 \times 10^{48}$ cm$^{-3}$ for the emitting region.

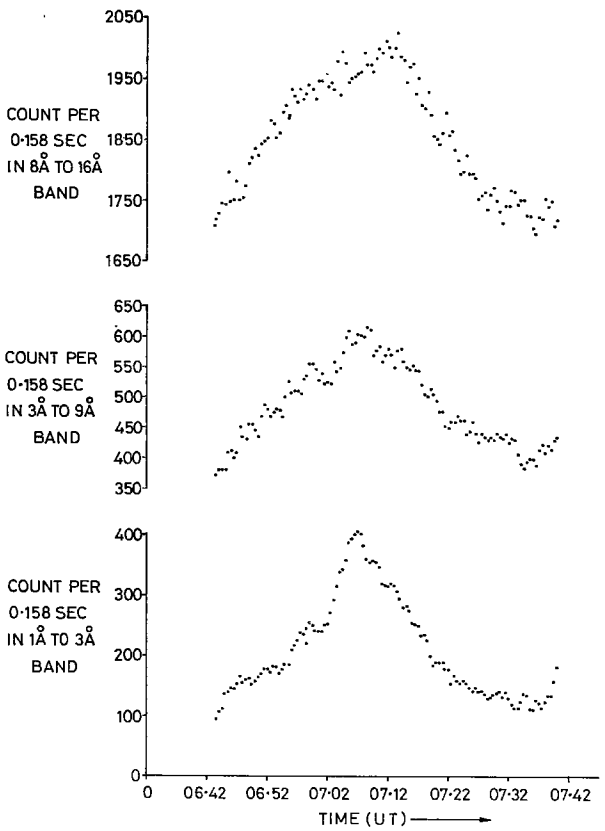


Fig. 16. Counting rates in 8–16 Å, 3–9 Å, and 1–3 Å bands plotted against time for a gradual rise and fall X-ray event on February 2, 1968.

The temperature increased from about $8.5 \times 10^6$ K to $11.5 \times 10^6$ K in a time of 20 min and returned to the lower value in about the same time. Such a temperature change in a region, optically *thin* at 2800 MHz and having the value of emission measure quoted above, would lead to a decrease in centimetre wave flux of $0.1 \times 10^{-22}$ W m$^{-2}$ Hz$^{-1}$. Such a small flux change would not be detectable. If the region were optically *thick* at centimetre wavelengths, the temperature increase of $2.8 \times 10^6$ K would lead to an increase of one flux unit at 2800 MHz in a region having an angular diameter of 0.5 arc min. No centimetre wave radio events were reported during the period of the X-ray event although at least two stations were observing at that time. The situation for this event in respect of radio activity is similar to that described for the precursor event in the previous section. The X-ray emitting region is either optically thin at centimetre wavelengths or, if optically thick, is less than 0.5 arc min in diameter. If these regions are optically thick, only a slightly larger temperature difference or a small increase in diameter would be required to produce a detectable microwave 'gradual rise and fall' event. Four X-ray events, that were correlated with 'gradual rise and fall' microwave events, exhibited slow rise times (see Figure 7). This would suggest that, at least on

some occasions, the X-ray emitting regions also emit microwave radiation. However, the number of events is very small and further comments must await the study of a larger number of 'gradual rise and fall' X-ray events.

In view of the slow rise and fall of the X-ray flux, the electrons in the emitting region should retain a Maxwellian velocity distribution throughout the event. If the emitting region has an electron density greater than $10^9$ cm$^{-3}$, the ion temperature should remain in equilibrium with the electron temperature (Spitzer, 1962), so the electrons will not lose energy by collisions with ions. It is possible that material is lost from the emitting region. Since the flux is never more than a factor two above the pre-event level, we cannot sensibly determine the emission measure throughout the falling part of the event and so are unable to check whether it is conserved. Unrestricted conduction of heat from the region would not allow the plasma to register any temperature increase although, as mentioned in 5.1, a special geometrical situation could permit a slow loss of energy due to thermal conduction. Finally, if radiative energy losses are responsible for cooling the region, we can estimate, from the rate of decrease of temperature, that the electron density is about $3 \times 10^{10}$ cm$^{-3}$. When combined with the emission measure, this value leads to a diameter of about 0.3 arc min for the emitting region and, assuming that the effective depth of the region is equal to its diameter, the optical depth at 2800 MHz is 0.7. This model of the region is therefore consistent with the absence of a microwave enhancement. However, the lack of spatial information for the X-ray emitting region means that several other models could also be valid. It is clear that simultaneous observations of the sizes and temperatures of the X-ray emitting regions would considerably limit the range of possible models.

## 6. Conclusions

From an examination of event profiles, we can divide the bursts into impulsive and gradual rise and fall categories. It is not possible to further sub-divide the impulsive classification on the basis of the observed event profiles. Since only events that were completely observable in a time of less than 60 min have been studied, there is a bias against gradual rise and fall events in the sample.

In the case of X-ray events that are correlated with microwave events, the X-ray emission is delayed by about 2 min with respect to the microwave peak. Among the X-ray detectors, the softer the radiation the later the time of peak flux. However, many X-ray events exhibit precursors and observations with the high sensitivity 1–3 Å detector usually show evidence of the start of X-ray activity well before the start of microwave activity.

There is a slight dependence of X-ray flux on flare area. X-ray events, originating in plage regions that are 'prolific' event producers, have peak fluxes greater than the average. There is no indication that X-ray burst peaks are delayed relative to the flare peaks. There is a just significant centre to limb decrease in the number of X-ray events that are correlated with H$\alpha$ flares.

Two impulsive events with different fall times were examined in detail. The falling

part of the X-ray flux cannot be explained by Bremsstrahlung from an electron beam with a power law energy spectrum. While the rising part of the events is not well fitted by a thermal continuum source function, this spectrum provides a better fit while the flux is decaying. Observation of the 1.9 Å Iron line during events with plasma temperatures less than $20.0 \times 10^6$ K suggests that some non-thermal process is exciting this line. Sizes and electron densities (see Table V) may be derived for the emitting regions if cooling models are assumed.

Many events are preceded by small flux enhancements or precursors. These small enhancements are due to temperature increases of less than $2.0 \times 10^6$ K. No increase in microwave radio flux was observed at the times of several precursors. This suggests that the source regions are either optically thin at microwave frequencies or, if optically thick, are smaller than 0.5 arc min in diameter. An average precursor spectrum was obtained by summing the count histograms obtained during the peak phases of seven events. Although the average temperature was $10.0 \times 10^6$ K, the Iron line to continuum ratio was found to be significant. The 1.9 Å line must therefore be excited non-thermally during precursor events.

Study of an X-ray gradual rise and fall burst showed a gradual temperature increase of $3.0 \times 10^6$ K during the event. No indication of the 1.9 Å Iron line was obtained. No corresponding microwave emission occurred during this event, but there is some evidence that gradual rise and fall X-ray and microwave events do occur together. In these cases the emitting regions must be optically thick at microwave frequencies.

The line observed during some events at around 1–9 Å cannot be due to the straightforward collisional excitation of the $1s^2$–$1s\,2p$ transition in $Fe^{+24}$. The observed temperatures are too low to permit the existence of sufficient $Fe^{+24}$ ions. The line may be produced by inner shell processes in stages below $Fe^{+22}$ (Blake, 1968).

It is also possible that the sudden release of energy in the initial phases of the events causes the population to differ markedly from that characteristic of a temperature at $10\text{-}15 \times 10^6$ K. The observed line could then be caused by collisional ionisation and dielectronic recombination in $Fe^{+24}$, but almost all the Iron in the emitting region would have to be in the $Fe^{+24}$ stage.

## Acknowledgements

Throughout the work we have benefited greatly from the support and encouragement of Professor R. L. F. Boyd. The assistance of many colleagues at University College London, Leicester University and Pye Laboratories of Cambridge is gratefully acknowledged. We also thank the National Aeronautics and Space Administration of the United States of America for providing the opportunity to fly an experiment on the Orbiting Solar Observatory. Throughout the programme we have been helped by the OSO Project Office and Ball Brothers Research Corporation who constructed the spacecraft. To them we extend our warmest thanks. Data reduction programmes were written by Mr. M. L. Shaw whose assistance was most valuable. We have benefited from discussions of the plasma cooling models with Dr. K. A. Pounds and

Dr. J. Vesecky. Dr. Carole Jordan suggested that dielectronic recombination could be important in exciting the $1s^2$–$1s\,2p$ transition in $Fe^{+24}$. Finally, we wish to acknowledge the contribution of Mrs. S. Ikes and Mrs. G. Willmore to the work of data reduction. The experiment was made possible by the financial support of the Science Research Council.

## References

Acton, L. W., Chubb, T. A., Kreplin, R. W., and Meekins, J. F.: 1963, *J. Geophys. Res.* **68**, 3335.
Arnoldy, R. L., Kane, S. R., and Winckler, J. R.: 1968, *Astrophys. J.* **151**, 711.
Blake, R. L.: 1968, Thesis, University of Colorado and High Altitude Observatory, NCAR Cooperative Thesis No. 15.
Covington, A. E.: 1959, *Paris Symposium on Radio Astronomy* (ed. by R. N. Bracewell), Stanford University Press, p. 159.
Culhane, J. L., Pounds, K. A., Sanford, P. W., and Willmore, A. P.: 1964, *Space Res.* **4**, 741.
Culhane, J. L., Sanford, P. W., Willmore, A. P., Blades, J., and Nettleship, R.: 1967, *I.E.E.E. Trans. Nucl. Sci.* **NS-14**, 38.
Culhane, J. L., Sanford, P. W., Shaw, M. L., Phillips, K. J. H., Willmore, A. P., Bowen, P. J., Pounds, K. A., and Smith, R. J.: 1969, *Monthly Notices Roy. Astron. Soc.* **145**, 435.
Culhane, J. L. and Phillips, K. J. H.: 1969, to be published in *Astrophys. J.*
De Jager, C.: 1964, paper presented at I.A.U. Symposium No. 23, Liège.
Donnelly, R. F.: 1968, E.S.S.A. Technical Report, ERL 81-SDL 2.
Friedman, H.: 1964, *AAS-NASA Symposium on the Physics of Solar Flares* (ed. by W. Hess), (Washington D.C. Scientific and Technical Information Division, NASA, Document No. SP-50), p. 147.
Fritz, G., Meekins, J. F., Henry, R. C., and Friedman, H.: 1969, *Astrophys. J. Letters* **156**, L33.
Frost, K.: 1964, *AAS-NASA Symposium on the Physics of Solar Flares* (ed. by W. Hess) (Washington D.C. Scientific and Technical Information Division, NASA, Document No. SP.-50), p. 139.
*Geophysics and Space Data Bulletin*: 1967, 1968, Vols. 4 and 5 (ed. by Norman J. Oliver and Anne L. Carrigan), Space Physics Laboratory, Air Force, Cambridge Research Laboratories.
Hudson, H. S., Peterson, L. E., and Schwartz, D. A.: 1969, *Astrophys. J.* **157**, 389.
Jordan, Carole: 1969, private communication.
Karzas, W. J. and Latter, R.: 1961, *Astrophys. J., Suppl. Ser.* **6**, 167.
Ken-Ichiro Ohki: 1969, *Solar Phys.* **7**, 260.
Kundu, M. R.: 1965, *Solar Radio Astronomy*, Interscience Publishers, New York.
Meekins, J. F., Kreplin, R. W., Chubb, T. A., and Friedman, H.: 1968, *Science* **162**, 891.
Neupert, W. M., White, W. A., Gates, W. J., Swartz, M., and Young, R. M.: 1969, *Solar Phys.* **6**, 183.
Peterson, L. E. and Winckler, J. R.: 1959, *J. Geophys. Res.* **64**, 697.
*Quarterly Bulletin of Solar Activity:* 1967, 1968, I.A.U. Eidgenössische Sternwarte, Zurich.
*Solar Geophysical Data*: 1967, 1968, U.S. Department of Commerce, Environmental Science Services Administration.
Spitzer, L.: 1962, *The Physics of Fully Ionised Gases*, 2nd edition, Interscience Publications, New York.
Takakura, T.: 1969, *Solar Phys.* **6**, 133.
Tanaka, H.: 1968, private communication.
Teske, R. G.: 1969, *Solar Phys.* **6**, 193.
Teske, R. G. and Thomas, R. J.: 1969, private communication.
Vaiana, G. S., Reidy, W. P., Zehnpfennig, T., Van Speybroeck, L., and Giaconni, R.: 1968, *Science* **161**, 564.
Van Allen, J. A.: 1967, *J. Geophys. Res.* **72**, 5903.
Vesecky, J.: 1969, private communication.
White, W. A.: 1964, *AAS-NASA Symposium on the Physics of Solar Flares* (ed. by W. Hess), (Washington D.C. Scientific and Technical Information Division, NASA, Document No. SP-50), p. 131.